

RESEARCH ARTICLE OPEN ACCESS

Alterations of Excitation–Inhibition Balance and Brain Network Dynamics Support Sensory Deprivation Theory in Presbycusis

Meixia Su¹  | Fuxin Ren¹ | Ning Li¹ | Fuyan Li¹ | Min Zhao¹ | Xin Hu¹ | Richard A. E. Edden^{2,3} | Muwei Li⁴  | Xiao Li¹ | Fei Gao¹ 

¹Department of Radiology, Shandong Provincial Hospital Affiliated to Shandong First Medical University, Jinan, China | ²Russell H. Morgan Department of Radiology and Radiological Science, The Johns Hopkins University School of Medicine, Baltimore, Maryland, USA | ³F. M. Kirby Research Center for Functional Brain Imaging, Kennedy Krieger Institute, Baltimore, Maryland, USA | ⁴Vanderbilt University Institute of Imaging Science, Nashville, Tennessee, USA

Correspondence: Xiao Li (lixiao55381026@sina.com) | Fei Gao (feigao@email.sdu.edu.cn)

Received: 20 March 2024 | **Revised:** 12 October 2024 | **Accepted:** 19 October 2024

Funding: This work was supported by the National Natural Science Foundation of China (Grant 81601479), Taishan Scholars Project of Shandong Province (Grant tstp20240525), Shandong Provincial Natural Science Foundation of China (Grants ZR2021MH030, ZR2021MH355), the Academic Promotion Programme of Shandong First Medical University (Grant 2019QL023), and Postdoctoral Innovation Projects of Shandong Province (No. SDCX-ZG-202400047). This work was also supported by National Institutes of Health (Grants R01 EB016089, R01 EB023963, R21 AG060245, P41 EB015909, and P41 EB031771).

Keywords: cognitive impairment | dynamic functional network connectivity | excitation–inhibition balance | GABA | presbycusis | sensory deprivation theory

ABSTRACT

Sensory deprivation theory is an important hypothesis involving potential pathways between hearing loss and cognitive impairment in patients with presbycusis. The theory suggests that prolonged auditory deprivation in presbycusis, including neural deaf-ferentation, cortical reallocation, and atrophy, causes long-lasting changes and reorganization in brain structure and function. However, neurophysiological changes underlying the cognition–ear link have not been explored. In this study, we recruited 98 presbycusis patients and 60 healthy controls and examined the differences between the two groups in gamma-aminobutyric acid (GABA) and glutamate (Glu) levels in bilateral auditory cortex, excitation–inhibition (E/I) balance (Glu/GABA ratio), dynamic functional network connectivity (dFNC), hearing ability and cognitive performance. Then, correlations with each other were investigated and variables with statistical significance were further analyzed using the PROCESS Macro in SPSS. GABA levels in right auditory cortex and Glu levels in bilateral auditory cortex were lower but E/I balance in right auditory cortex were higher in presbycusis patients compared to healthy controls. Hearing assessments and cognitive performance were worse in presbycusis patients. Three recurring connectivity states were identified after dFNC analysis: State 1 (least frequent, middle-high dFNC strength with negative functional connectivity), State 2 (high dFNC strength), and State 3 (most frequent, low dFNC strength). The occurrence and dwell time of State 3 were higher, on the other hand, the dwell time of State 2 decreased in patients with presbycusis compared to healthy controls. In patients with presbycusis, worse hearing assessments and cognition were correlated with decreased GABA levels, increased E/I balance, and aberrant dFNC, decreased GABA levels and increased E/I balance

Abbreviations: AVLT, Auditory Verbal Learning Test; BOLD, blood oxygenation level dependent; CSF, cerebrospinal fluid; dFNC, dynamic functional network connectivity; E/I, excitation–inhibition; GABA, gamma-aminobutyric acid; Glu, glutamate; GM, gray matter; HC, healthy controls; PC, presbycusis; PTA, pure tone average; rs-fMRI, resting-state functional MRI; WM, white matter

The first two authors contributed equally to this work.

This is an open access article under the terms of the [Creative Commons Attribution-NonCommercial-NoDerivs](https://creativecommons.org/licenses/by-nc-nd/4.0/) License, which permits use and distribution in any medium, provided the original work is properly cited, the use is non-commercial and no modifications or adaptations are made.

© 2024 The Author(s). *Human Brain Mapping* published by Wiley Periodicals LLC.

were correlated with decreased occurrence and dwell time in State 3. In the mediation model, the fractional windows, as well as dwell time in State 3, mediated the relationship between the E/I balance in right auditory cortex and episodic memory (Auditory Verbal Learning Test, AVLT) in presbycusis. Moreover, in patients with presbycusis, we found that worse hearing loss contribute to lower GABA levels, higher E/I balance, and further impact aberrant dFNC, which caused lower AVLT scores. Overall, the results suggest that a shift in E/I balance in right auditory cortex plays an important role in cognition-ear link reorganization and provide evidence for sensory deprivation theory, enhancing our understanding the connection between neurophysiological changes and cognitive impairment in presbycusis. In presbycusis patients, E/I balance may serve as a potential neuroimaging marker for exploring and predicting cognitive impairment.

1 | Introduction

Age related hearing loss (ARHL), also known as presbycusis, primarily manifests as decreased high-frequency auditory perception and compromised speech recognition especially in noisy environments (Gates and Mills 2005) and seriously affects daily communication and social interactions. It ranks the third most prevalent health condition among the elderly after only heart disease and arthritis, and about 65% of people over the age of 60 suffer from hearing loss of different degrees (Lin and Albert 2014). ARHL also affects mental health, leading to anxiety, stress, and depression, and even cognitive impairment. Even minor degrees of hearing loss may increase the long-term risk of cognitive decline and dementia (Albers et al. 2015). Although many studies have highlighted the close association between ARHL and cognitive decline or elevated risk of dementia (Loughrey et al. 2018), the exact neural mechanisms responsible for cognitive impairment is the subject of ongoing investigation.

Numerous magnetic resonance imaging (MRI) studies of presbycusis patients have reported alterations in brain structure. For example, a longitudinal study showed that, compared with total brain atrophy, high-frequency hearing loss in patients with presbycusis was related to an imbalance of temporal lobe atrophy and Minimum Mental State Examination (MMSE) score was related to frontoparietal lobe atrophy (Qian et al. 2017). Another study found that in presbycusis patients with cochlear dysfunction, the Nomination (Boston) score, which is widely used to assess visual confrontation naming and picture descriptions, was directly related to the volume of the left orbitofrontal, right thalamus, bilateral hippocampus, anterior cingulate gyrus, and insula (Belkhiria et al. 2020). A resting-state functional MRI (rs-fMRI) study demonstrated that the directional functional connection between the middle temporal gyrus, insular lobe, and hippocampus was reduced in presbycusis patients (Chen et al. 2019). With increasing hearing loss, functional network connectivity (FNC) of the dorsal attention network to sensorimotor and primary motor cortex, as well as the connection between the salience network and visual cortex decreased (Schulte et al. 2020).

Recent studies have shown that the characteristics of spontaneous brain activity and regional interconnections (FNC) change in a short period of time and they are related to changes in cognitive function in schizophrenia and Parkinson's disease (PD) (Chang and Glover 2010; Damaraju et al. 2014; Kim et al. 2017; Xie et al. 2019). Utilizing rs-fMRI, the dFNC method enables examination of the evolving properties of diverse brain networks or components estimated through spatial independent component analysis (sICA) (Sakoğlu et al. 2010). Unlike

rs-fMRI, which emphasizes the average strongest and most stable modes or functional interactions over time, dFNC examines the characteristics of FNC changes over periods of seconds to minutes (Chen, Rubinov, and Chang 2017) to explain time-varying and dynamic information interactions to reveal the complex and changeable characteristics and mechanisms of brain networks. Studies applying dFNC to study PD and schizophrenia patients have reported changes in connectivity between different networks (Damaraju et al. 2014; Fiorenzato et al. 2019; Kim et al. 2017), revealing changes in the separation and integration of brain functions and demonstrating that dFNC can provide more information about the functional network connections. However, dFNC has rarely been applied to study cognitive impairment in presbycusis.

Gamma-aminobutyric acid (GABA) and glutamate (Glu), as the main excitatory and inhibitory neurotransmitters, play essential roles in the central auditory system. Early investigations reported a significant reduction in the expression of glutamate dehydrogenase (GAD) and GABA receptor proteins within the central nucleus of the inferior colliculus and auditory cortex in aging Fischer-344 rats (Casparly et al. 1990; Tang et al. 2014). This age-related decrease in GAD may reflect a decrease in metabolism and presynaptic GABA levels, indicating the plasticity of inhibitory GABA neurotransmission is downregulated. By the method of edited magnetic resonance spectroscopy termed Mescher–Garwood point-resolved spectroscopy sequence (MEGA-PRESS), patients with presbycusis demonstrated a distinct decrease in GABA levels in auditory cortex. Importantly, the degree of hearing loss exhibited a strong correlation with GABA levels (Gao et al. 2015; Li et al. 2023). Another MEGA-PRESS investigation established a connection between reduced GABA levels in auditory area and cognitive decline in elderly adults, suggesting that neural de-differentiation may affected by auditory GABA levels (Lalwani et al. 2019). Considering the glutamatergic and GABAergic systems are altered in presbycusis, it is likely that these neurotransmitters systems, especially excitation–inhibition (E/I) balance (Glu/GABA ratio), contribute to any alterations observed in dFNC.

In the present study, we utilized edited magnetic resonance spectroscopy (MRS) and rs-fMRI to examine changes in auditory neurotransmitter levels and dFNC in patients with presbycusis. Informed by previous findings, the relationships between hearing loss, cognitive function, MRS, and dFNC were analyzed to evaluate the following: (1) changes in neurotransmitter levels and dFNC between presbycusis patients and controls; (2) correlations between hearing loss, neurotransmitter levels, and dynamic features of functional connectivity and cognitive impairment in PC group; and (3) the mediate role of E/I balance

and dFNC characteristics in the link from hearing loss to cognitive impairment in presbycusis.

2 | Materials and Methods

2.1 | Participants

The subjects' consent was obtained according to the Declaration of Helsinki and this study was approved by the Research Ethics Board for Shandong Provincial Hospital Affiliated to Shandong First Medical University. We enrolled a total of 98 presbycusis patients (PC group; 53 males and 45 females) with a mean age of 65.65 ± 3.27 years, and 60 healthy controls (HC) group (31 males and 29 females) with a mean age of 65.4 ± 2.29 years. All participants in the PC group were age 60 or older with an average pure tone average (PTA) > 25 dB HL at 0.5, 1, 2, and 4 kHz (air conduction) in their better hearing ear (Lin et al. 2011). The exclusion criteria were as follows: (1) any ear disease affecting the hearing threshold, such as tinnitus, hyperacusis, or Meniere's disease; (2) a history of otologic surgery, ototoxic drug therapy, noise exposure, or hearing aid use; (3) asymmetrical hearing loss with a difference of > 20 dB in at least two frequencies; (4) neurological or psychiatric disease; and (5) contraindications to MRI. Participants in the HC group were age- and gender-matched with the PC group and all in good health with a PTA of 25 dB HL or less in the better hearing ear. All participants were right-handed. None of the participants had a career in sound or a history of severe smoking or alcoholism.

2.2 | Neuropsychological Assessment

The evaluation of cognitive functions across various domains was performed in a predetermined sequence after MRI scanning and took approximately 1 h. The sequence commenced with the Montreal Cognitive Assessment (MoCA) (Lu et al. 2011) to assess general cognitive function. The Hospital Anxiety and Depression Scale (HADS) (Zigmond and Snaith 1983) was then administered to assess anxiety and depression symptoms. Episodic verbal learning and recall was assessed using the Auditory Verbal Learning Test (AVLT) (Zhao et al. 2012). Next, the Symbol Digit Modalities Test (SDMT) (Schepondom et al. 2014) and Stroop color word interference test (Stroop) (Savitz and Jansen 2003) were performed to assess mental processing speed and visuospatial abilities. Lastly, executive control was assessed by the Trail Making Test A and B (TMT-A and TMT-B) (Sánchez-Cubillo et al. 2009).

2.3 | MRI Acquisition

All the data, including T1WI sequence, rs-fMRI, and MRS data, were acquired using an eight-channel phased-array head coil within a 3.0T Philips Achieva TX scanner. A three-dimensional turbo fast echo (3D-TFE) T1WI sequence was used to obtain brain structural images with the following parameters: repetition time (TR)=8.1 ms, echo time (TE)=3.7 ms, inversion time (TI)=1027 ms, voxel size= $1 \times 1 \times 1$ mm³, field

of view= 24×24 cm², slice thickness=1 mm, and 160 slices. Resting-state blood oxygenation level dependent (BOLD) data were collected using a gradient-echo echo-planar imaging (EPI) sequence with the following parameters: TR=2000 ms; TE=35 ms; field of view= 24×24 cm²; in-plane resolution= 3.75×3.75 mm²; slice thickness=4 mm; 35 slices; and a total of 240 volumes. Bilateral Heschl's gyri (Figure 1) with a voxel size of $4.0 \times 2.0 \times 2.0$ cm³ were selected as the volumes of interest (VOI) to obtain edited-GABA data using the macromolecule (MM)-suppressed MEGA-PRESS sequence with the following parameters: TR/TE=2000/80 ms; bandwidth=2000 Hz; "ON/OFF" editing pulses=1.9/1.5 ppm; and a total of 320 averages (Harris et al. 2015). Glu data were obtained using PRESS sequence with the following parameters: TR/TE=2000/35 ms; bandwidth=2000 Hz; and a total of 64 averages. Water suppression was performed using Chemical Shift Selective Suppression (CHESS). Prior to each acquisition, FASTMAP shimming was automatically executed. Shorter measurements with eight averages were employed to acquire unsuppressed water data. A T2-weighted fluid-attenuated inversion recovery (T2-FLAIR) sequence was used to assess white matter (WM) abnormal hyperintensity and intracranial lesions.

2.4 | Rs-fMRI Data Processing and Dynamic Functional Network Connectivity

Structural and functional MRI data were preprocessed using the Data Processing & Analysis for Brain Imaging (DPABI) V5.1 toolbox (Chao-Gan et al. 2016) and SPM12 software. First, for rs-fMRI data, the first 10 volumes of all 240 dynamics were removed to allow participants' adaptation to the environment and equilibration effects. Subsequently, the data were corrected by slice-timing and realignment analysis for head motion correction. Head movements greater than 2 mm and 2° were removed. Rs-fMRI images were first linearly co-registered to the 3D-T1W image of the same subject and segmented into gray matter (GM), WM, and cerebrospinal fluid (CSF). Next, the segmented spatial parameters were spatially normalized in Montreal Neurological Institute (MNI) space using nonlinear transformations and resampled to 3 mm³ isotropic voxels. Finally, the data underwent nuisance covariate regression incorporating the Friston 24 head motion parameters (Karl et al. 1996), WM and CSF signal. Further preprocessing steps included linear detrending, temporal filtering within the frequency range of 0.01–0.08 Hz and smoothing with an isotropic Gaussian kernel (full-width at half-maximum [FWHM]=4 mm).

Group independent component analysis (Group ICA) was carried out by Group ICA of functional MRI Toolbox (GIFT <http://icatb.sourceforge.net>). All participants' data were decomposed into functional networks with a unique course profile, and went subject-specific and group-level reductions steps. For subject-specific step, data were reduced by the principal component analysis and concatenated across time. At group-level step, the subject-specific data were extracted with the expectation-maximization algorithm and 100 independent components were identified. The ICA algorithm was repeated 20 times in ICASSO implemented in GIFT to ensure the reliability and stability. Then independent components with cluster

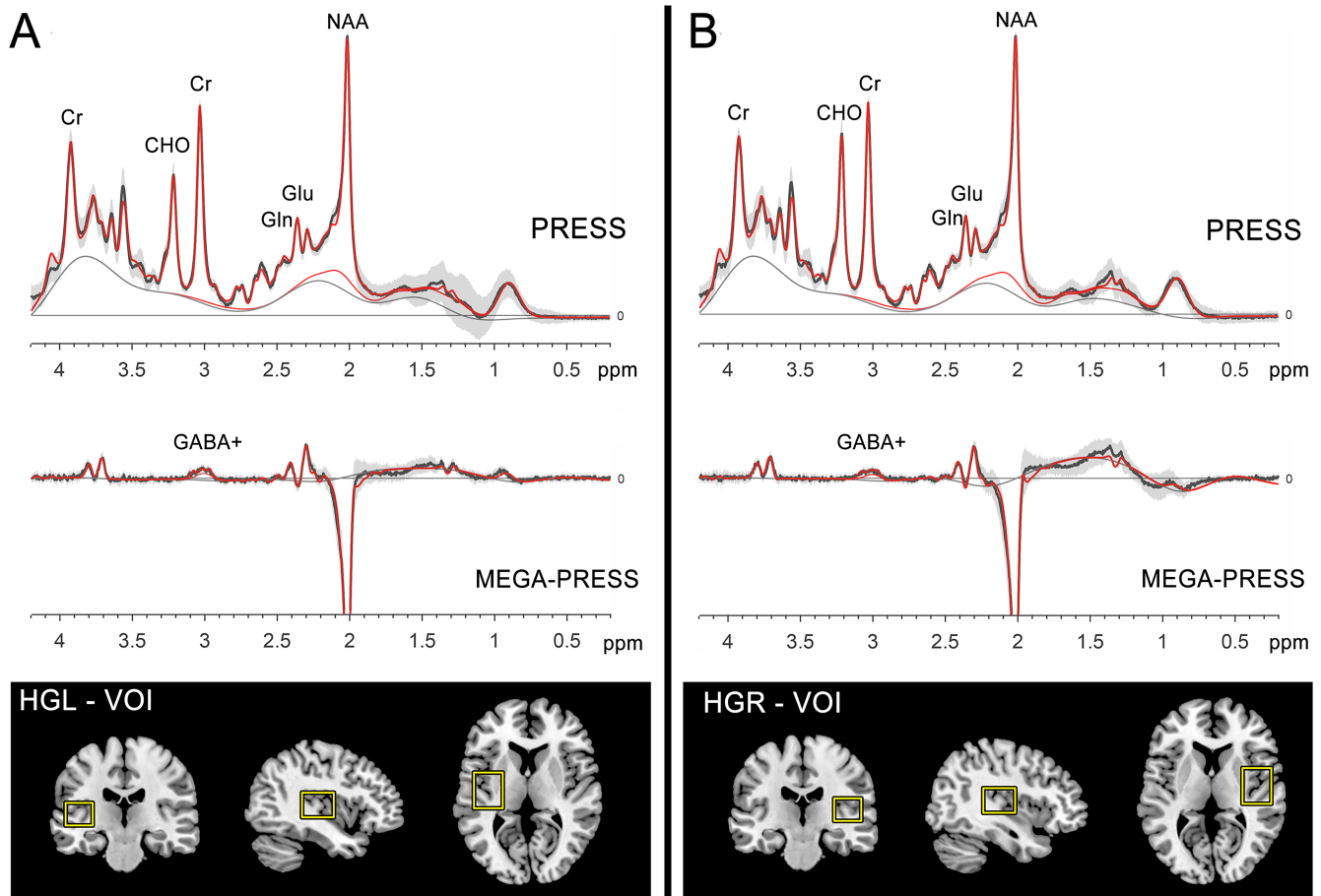


FIGURE 1 | Average MM-suppressed MEGA-PRESS and PRESS spectra and VOI in both right (A) and left (B) auditory region are depicted. MEGA-PRESS: Mescher–Garwood point-resolved spectroscopy sequence, MM: macromolecules.

stability/quality (I_q) index > 0.8 were selected. Subject-specific spatial maps and time courses were back-projected using the GICA back-reconstruction approach (Calhoun et al. 2001). Finally, 26 independent components (Figure 2) were selected based on the criteria by Allen et al. (2014) and they were divided into seven networks spatial according to the correlation values between independent components and the template (Shirer et al. 2012), including subcortical (SN), cerebellar (CB), auditory network (AN), visual network (VN), sensorimotor network (SMN), default mode network (DMN), and cognitive executive network (CEN). Z-score transformation was performed for visualization.

A sliding time window approach was used to calculate the time-varying correlations within the 26 independent component networks in the GIFT software package. To provide a good compromise between the quality of correlation matrix estimation and the ability to resolve dynamics, the sliding time window along the 230-TR length scan was set with window size = 30 TRs, step = 1 TR, Gaussian window alpha = 3 TRs, number of repetitions (L1 regularization) = 10 (Leonardi and Van De Ville 2015), resulting in 199 consecutive windows with 26×26 pairwise covariance matrix.

K-means clustering of the dFNC matrices for each participant was used to extract reoccurring functional connectivity

patterns (states). To decrease redundancy between windows and computational demands, an initial clustering on a subset of windows (consisting of local maxima in functional connectivity variance) from each subject was performed. The number of clusters was determined based on the elbow criterion, which is calculated as the ratio of within-cluster to between-cluster distances, ultimately leading to selection of three clusters. Finally, these three subject centroids as subject exemplars were used as an initial point to cluster all subjects' dFNC windows.

For the analysis of strength in dFNC, Fisher's z-transformation was applied to transform all functional connectivity matrices into z-scores to enhance the normality of Pearson's r distribution. The mean dFNC correlations ($26 \times 25/2$) in each of the three states were compared with two-sample t -tests, with a significance threshold of $p < 0.05$ (FDR corrected). For the analysis of temporal properties in dFNC, three dFNC indices in the participants' state transition vector were evaluated. Fractional windows represented the percentage of windows belonging to one state of all states. Mean dwell time represented the average number of consecutive windows belonging to one state before switching to another. The number of transitions represented the count of transitions between different states and is also the reliability over time. Two-sample t -test was used to examine the group difference with a significance threshold of $p < 0.05$ (FDR corrected).

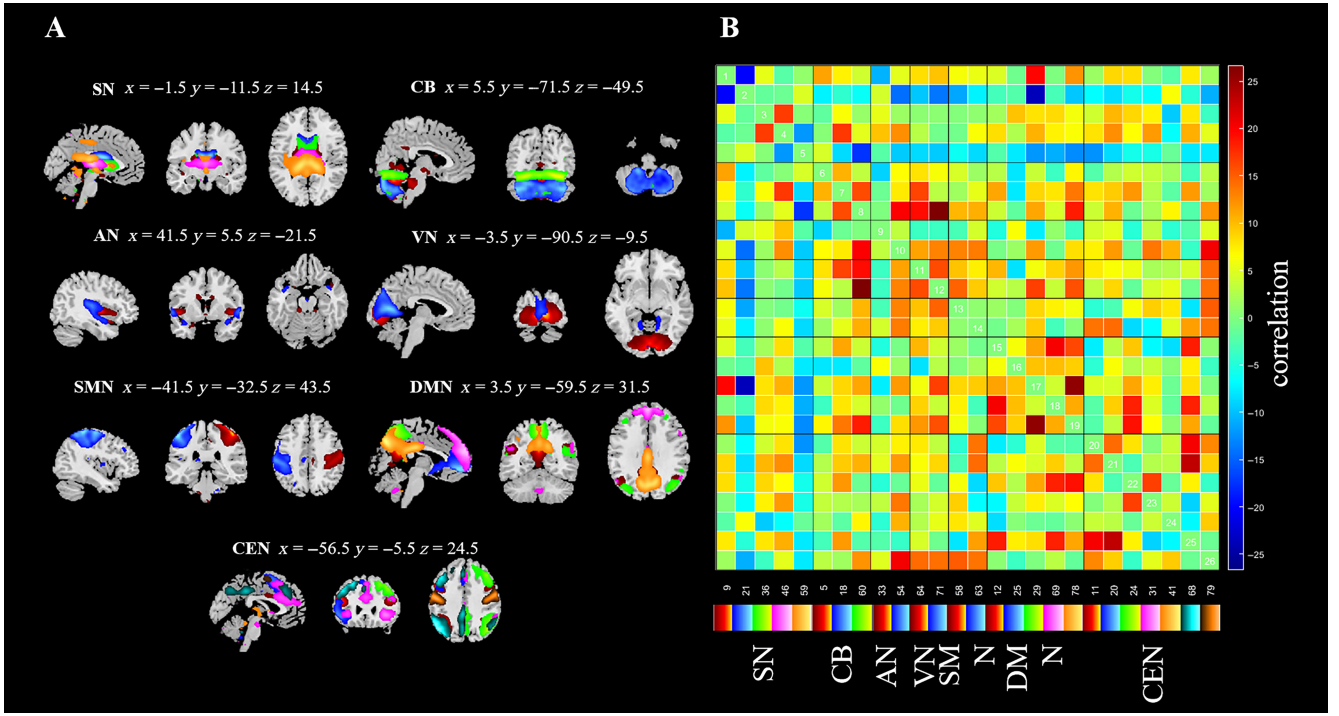


FIGURE 2 | The 26 independent components identified by a group ICA. (A) The 26 independent components and their spatial distribution. (B) 26 independent components were rearranged into seven functional networks. Pearson correlation coefficient were transformed to z-score (the correlation value) using Fisher's z-transformation. The color-coded legend under the matrix was matched with the overlaid colors of the spatial maps in (A). AN: auditory network, CB: cerebellar, CEN: cognitive executive network, DMN: default mode network, SMN: sensorimotor network, SN: subcortical, VN: visual network.

2.5 | MRS Data Analysis

To quantify GABA levels we applied MM-suppressed MEGA-PRESS data in Gannet 3.1 (Edden et al. 2012). To ensure accurate fitting of the GABA peaks at 3 ppm, a Gaussian curve and 3 Hz line broadening were used. Glu levels were determined by analyzing PRESS data with the LC Model (version 6.3-1 M) (Provencher 1993).

Subsequently, Gannet was employed to co-register the MRS VOIs with 3D T1-weighted data and then segment them into GM, WM, and CSF. To ensure data quality, we only considered spectra with GABA fitting errors < 20% and Cramer-Rao lower bounds (CRLB) of Glu < 20% for further analysis. We performed corrections for metabolite levels by considering T1 and T2 relaxation times, along with addressing partial volume effects. Following this correction, we calculated metabolite levels in institutional units (i.u.) on a water-scaled basis using the formula (Gasparovic et al. 2006; Mullins et al. 2014) as follows:

$$[\text{GABA}] = \frac{S_{\text{GABA}}}{R_{\text{GABA}}} \times [\text{H}_2\text{O}] \times \frac{f_{\text{GM}} \times R_{\text{H}_2\text{O_GM}} + f_{\text{WM}} \times R_{\text{H}_2\text{O_WM}} + f_{\text{CSF}} \times R_{\text{H}_2\text{O_CSF}}}{S_{\text{H}_2\text{O}} \times (1 - f_{\text{CSF}}) \times k} \quad (1)$$

$$[\text{Glu}] = \frac{S_{\text{Glu}}}{R_{\text{Glu}}} \times [\text{H}_2\text{O}] \times \frac{f_{\text{GM}} \times R_{\text{H}_2\text{O_GM}} + f_{\text{WM}} \times R_{\text{H}_2\text{O_WM}} + f_{\text{CSF}} \times R_{\text{H}_2\text{O_CSF}}}{S_{\text{H}_2\text{O}} \times (1 - f_{\text{CSF}})} \quad (2)$$

The signal integrals of GABA denoted as S_{GABA} , Glu denoted as S_{Glu} , and water denoted as $S_{\text{H}_2\text{O}}$ were defined by Gannet (Edden et al. 2014) and LC Model (Bartos, Vida, and Jonas 2007). The concentration of pure water ($[\text{H}_2\text{O}]$) was set at 55,550 mmol/kg. The fractions of water associated with GM, WM, and CSF, were represented by f_{GM} , f_{WM} , and f_{CSF} (Gasparovic et al. 2006). We defined the editing efficiency for MEGA-PRESS (k) as 0.5. The following equation was used to accommodate relaxation attenuation: $R_{\text{H}_2\text{O_y}} = \exp[-\text{TE}/T2_{\text{w_y}}] (1 - \exp[-\text{TR}/T1_{\text{w_y}}])$, in which $T1$ relaxation time of water in compartments y (GM, WM, or CSF) denoted as $T1_{\text{w_y}}$ and $T2$ relaxation time denoted as $T2_{\text{w_y}}$. The GABA relaxation attenuation factor was described as R_{GABA} , and the Glu, was described as R_{Glu} . In this study, the relaxation times applied were as follows: water in GM, $T1/T2 = 1331/110$ ms; water in WM, $T1/T2 = 832/79.2$ ms; CSF, $T1/T2 = 3817/503$ ms (Lu et al. 2005; Piechnik et al. 2009; Wansapura et al. 1999); GABA, $T1/T2 = 1310/88$ ms (Edden et al. 2012; Puts, Barker, and Edden 2013); and Glu, $T1/T2 = 1270/181$ ms (Ganji et al. 2012; Mlynarik, Gruber, and Moser 2001). E/I balance was obtained by calculating the Glu to GABA ratio.

2.6 | Statistical Analysis

Statistical analyses were performed using SPSS 12 (IBM, USA). Student's t -test was used to compare continuous variables including age, education, hearing, and cognitive assessments between the HC and PC groups, while categorical variables including gender were compared using Pearson's chi-squared test. Subsequently, the comparison of dFNC characteristics

were described in Section 2.4. Shapiro–Wilk tests were used to examine the data distribution and Pearson’s or Spearman’s correlation analysis was used to examine relationships between altered neurotransmitter levels, temporal properties, and neuropsychological test scores. The above variables were normally distributed. FDR correction was used for multiple comparisons and the threshold for statistical significance was set at $p \leq 0.05$.

Data with significant differences between the HC and PC groups in metabolite levels, dFNC, cognitive function, and hearing assessment scores (as detailed in the Results) were further analyzed using the PROCESS Macro in SPSS (Hayes 2017). Simple mediation models were constructed to explore the link between E/I balance and cognitive function with dFNC as a potential mediator and age, gender, and education level included as covariates. Serial mediation models were also tested for the parallel and serial mediating effects of metabolite level and dFNC on the relationship between hearing loss and cognitive function.

3 | Results

3.1 | Participant Characteristics

The clinical, hearing assessments, and neuropsychological characteristics of 60 HCs and 98 PC patients are presented in Table 1. There were no statistically significant group differences in demographic factors such as sex, age, and education level ($p > 0.05$,

Table 1). PC group had a worse auditory performance than HC group, with higher PTA and speech reception threshold (SRT) (all $p < 0.001$, Table 1). The PC group performed significantly worse on the cognitive assessment, as indicated by lower MoCA, AVLT, and SDMT scores, and higher Stroop, TMT-A, and TMT-B scores ($p < 0.01$, Table 1). Besides, there were no statistically significant group differences in assessments related to anxiety and depression.

3.2 | Comparison of Auditory Cortex Metabolite Levels and E/I Balance

Significant differences were not observed in the GM or WM fractions in bilateral auditory cortex in the two groups ($p > 0.05$, Table 2). As described in the methods, no participants were excluded based on fitting errors or CRLB. Similarly, when comparing the fitting errors or CRLB values in HC and PC groups, there were no significant disparities ($p > 0.05$, Table 2). Notably, GABA levels in the PC group were reduced in the right auditory cortex compared to the HC group ($t = 4.2$, $p < 0.001$), but in the left auditory cortex, no significant differences were detected ($t = 1.229$, $p = 0.221$). Glu levels decreased in the PC group compared with HC group in both the left ($t = 3.349$, $p = 0.001$) and right ($t = 2.681$, $p = 0.012$) auditory cortex (Table 2). In more detailed analyses, no notable distinctions between the two groups were observed in E/I balance in the left auditory cortex ($t = -0.638$, $p = 0.542$). However, the E/I balance of the right auditory cortex in the PC group differed significantly from that of the HC group ($t = -2.534$, $p = 0.012$). There was no correlation in

TABLE 1 | Demographics of PC group and the HC group.

	HC group (<i>n</i> = 60)	PC group (<i>n</i> = 98)	χ^2/t -value	df	<i>p</i>
Age (year)	65.4 ± 2.29	65.65 ± 3.27	0.293	152.986	0.569
Gender (male/female)	31/29	53/45	0.087	1	0.768
Education (years)	11.35 ± 3.22	11.23 ± 2.56	0.249	156	0.804
PTA (dB HL)	11.17 ± 3.83	36.73 ± 10.31	-22.181	134.436	< 0.001***
SRT (dB HL)	11.47 ± 4.19	36.69 ± 12.67	-18.148	128.076	< 0.001***
MoCA	26.85 ± 1.98	25.58 ± 2.14	3.718	156	< 0.001***
Anxiety	3.58 ± 3.33	3.28 ± 3.11	0.587	156	0.558
Depression	3.6 ± 3.52	3.91 ± 3.52	-0.534	156	0.594
AVLT	52.18 ± 11.71	45.31 ± 10.63	3.797	156	< 0.001***
SDMT	33.2 ± 12.48	24.19 ± 11.51	4.623	156	< 0.001***
Stroop	138 ± 36.48	163.84 ± 50.79	-3.710	151.955	< 0.001***
TMT_A	57.7 ± 23.29	78.25 ± 34.11	-4.114	156	< 0.001***
TMT_B	176.03 ± 79.48	225.74 ± 91.41	-3.482	156	0.001**

Note: Quantitative variables are represented as mean ± standard deviation (SD). *p*-value for gender was derived using chi-squared test (two-tailed), for others using two-sample *t*-tests (two-tailed).

Abbreviations: AVLT, Auditory Verbal Learning Test; HC, health control; MoCA, Montreal Cognitive Assessment; PC, patients with presbycusis; PTA, pure tone audiometry; SDMT, Symbol Digit Modalities Test; SRT, speech reception threshold; Stroop, Stroop color word interference test; TMT, Trail Making Test.

*** $p < 0.001$.

** $p < 0.01$.

TABLE 2 | Comparison of MRS data between PC group and HC group.

Characteristics	HC group	PC group	<i>t</i> -value	df	<i>p</i>
Left					
GABA levels (i.u.)	1.05 ± 0.27	0.99 ± 0.34	1.229	156	0.221
GABA fitting errors	10.07 ± 3.21	10.07 ± 3.27	0.011	156	0.991
GMF (%)	50.47 ± 5.35	49.75 ± 5.12	0.85	156	0.397
WMF (%)	30.97 ± 8.31	32.04 ± 6.90	-0.874	156	0.384
Glu levels (i.u.)	9.26 ± 0.94	8.71 ± 1.05	3.349	156	0.001**
Glu CRLB	6.02 ± 0.83	6.15 ± 1.33	-0.794	155.874	0.429
EI balance	9.56 ± 3.4	9.99 ± 4.49	-0.638	156	0.524
Right					
GABA levels (i.u.)	1.29 ± 0.29	1.11 ± 0.23	4.2	103.37	<0.001***
GABA fitting errors	9.58 ± 2.85	9.8 ± 3.21	-0.423	156	0.673
GMF (%)	50.89 ± 4.81	50.43 ± 5.87	0.513	156	0.609
WMF (%)	30.71 ± 7.85	31.66 ± 6.71	-0.805	156	0.422
Glu levels (i.u.)	9.7 ± 1.08	9.26 ± 0.98	2.681	156	0.008*
Glu CRLB	5.75 ± 0.6	5.78 ± 0.83	-0.207	156	0.836
EI balance	7.84 ± 1.8	8.78 ± 2.48	-2.534	156	0.012*

Note: The MRS data is represented as mean ± standard deviation (SD). *p*-value was derived using two-sample *t*-tests (two-tailed).

Abbreviations: CRLB, Cramer–Rao lower bound; EI, excitation–inhibition; GABA, gamma-aminobutyric acid; Glu, glutamate; GMF, gray matter fractions; HC, health control; PC, patients with presbycusis; WMF, white matter fractions.

****p* < 0.001.

***p* < 0.01.

**p* < 0.05.

bilateral auditory cortex between Glu and GABA levels in the HC or PC groups.

in the connectivity strength of each state at various regional pairings.

3.3 | dFNC Analysis

Dynamic changes in FNC over time were subjected to *k*-means clustering, resulting in the segmentation of all participants into three distinct states (Figure 3A): State 1 (least frequent, middle-high dFNC strength with negative functional connectivity), State 2 (high dFNC strength), and State 3 (most frequent, low dFNC strength). Notably, not all participants transitioned through all states. As shown in Figure 3B, State 3 was more frequently observed in the PC group than in the HC group ($t = -2.529$, $p = 0.039$, FDR corrected). However, there were no significant group differences in the occurrences of State 1 ($t = 1.088$, $p = 0.278$, FDR corrected) or State 2 ($t = 1.481$, $p = 0.212$, FDR corrected) in the fractional windows. The mean dwell time in State 1 did not differ significantly between the HC and PC groups ($t = 0.252$, $p = 0.802$, FDR corrected) in Figure 3C. However, the PC group exhibited a shorter mean dwell time in State 2 than the HC group ($t = 2.408$, $p = 0.027$, FDR corrected). In contrast, the PC group showed a longer mean dwell time in State 3 compared to the HC group ($t = -3.765$, $p = 0.003$, FDR corrected). No differences were observed between the HC and PC groups in the number of transitions ($t = 0.759$, $p = 0.723$) in Figure 3D. There were no significant group disparities between the HC and PC groups

3.4 | Correlations Between Hearing Assessment, Metabolite Levels, dFNC, and Cognitive Function

In Figure 4, right auditory GABA levels were positively correlated with AVLT scores ($r = 0.4958$, $p < 0.05$) but negatively correlated with TMT-A scores ($r = -0.3966$, $p < 0.05$) and TMT_B ($r = -0.2818$, $p < 0.05$) in the PC group. However, E/I in right auditory cortex (E/I-R) were negatively related to AVLT scores ($r = -0.4137$, $p < 0.001$) but positively related to TMT-A scores ($r = 0.4553$, $p < 0.05$) and TMT_B ($r = 0.3035$, $p < 0.05$). Right auditory GABA levels were positively correlated with fractional windows in State 3 ($r = 0.4627$, $p < 0.05$) and the dwell time in State 3 ($r = 0.4604$, $p < 0.05$) in the PC group. On the contrary, E/I-R were negatively correlated with fractional windows in State 3 ($r = -0.3568$, $p < 0.05$) and the dwell time in State 3 ($r = -0.3419$, $p < 0.05$) in the PC group. There was also a positive relationship between the fractional windows in State 3 and AVLT scores ($r = 0.4032$, $p < 0.05$), same as observed between the dwell time in State 3 and AVLT scores ($r = 0.3584$, $p < 0.05$). The relationship between dwell time in State 3 and TMT-A was negative ($r = -0.3061$, $p < 0.05$). GABA levels in the right auditory cortex were negatively correlated with both PTA scores ($r = -0.5078$, $p < 0.05$) and SRT ($r = -0.4604$, $p < 0.05$) in the PC group. Conversely, E/I-R exhibited a positive correlation with

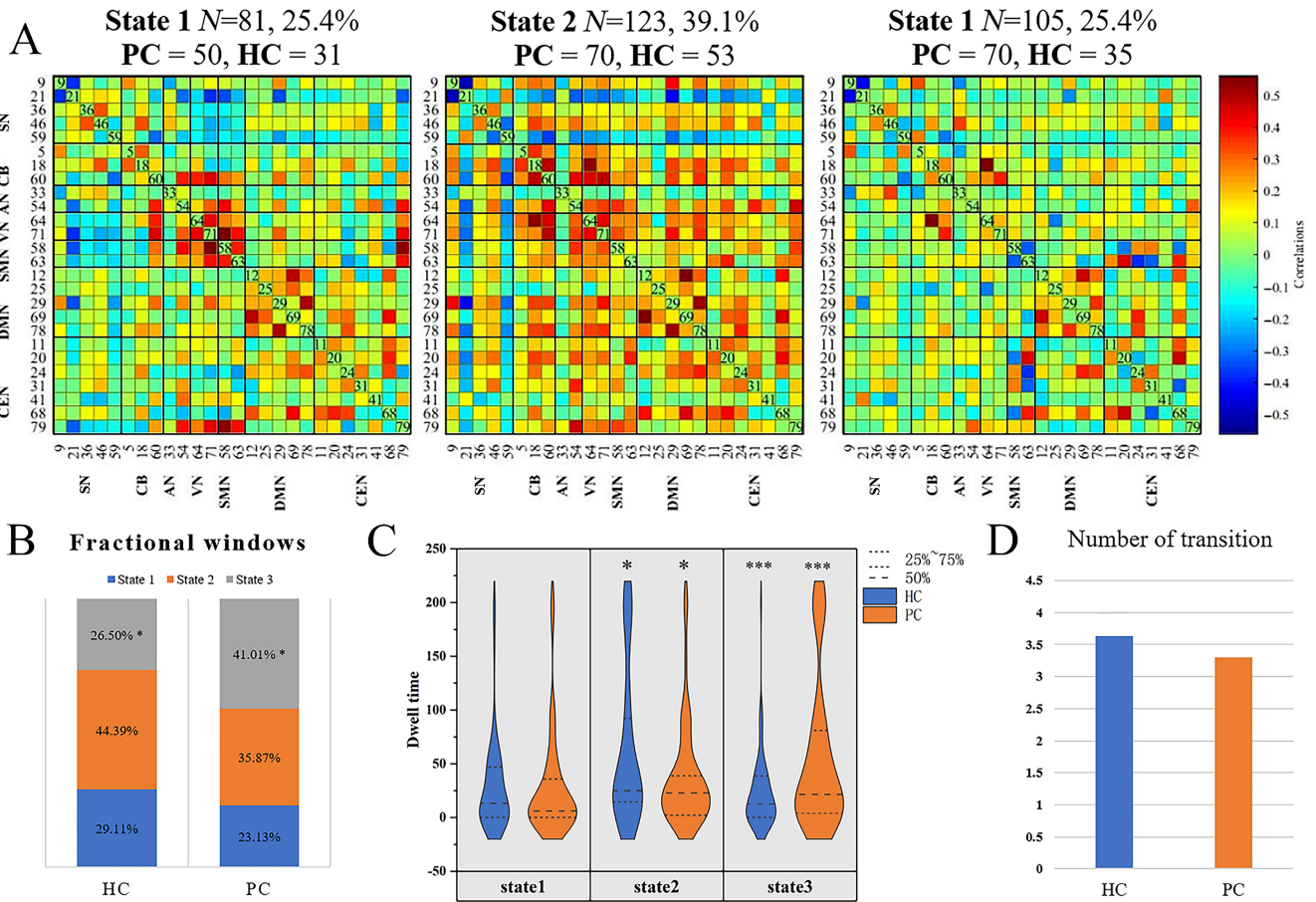


FIGURE 3 | Cluster centroids for each state in the upper row and temporal properties of FNC state analysis in the lower row. (A) The total number of subjects, the percentage of occurrence in each state were above the picture. The fractional windows (B) (the percentage of windows belonging to one state), dwell time (C) (the average number of consecutive windows belonging to one state before switching to another), and the number of transitions (D) (the count of transitions between different states) is depicted for healthy controls (HC) and patients with presbycusis (PC). AN: auditory network, CB: cerebellar, CEN: cognitive executive network, DMN: default mode network, SMN: sensorimotor network, SN: subcortical, VN: visual network. *** $p < 0.001$, * $p < 0.05$.

PTA ($r = 0.5310$, $p < 0.05$) scores and SRT ($r = 0.4667$, $p < 0.05$). The fractional windows in State 3 was negatively correlated with PTA ($r = -0.2534$, $p < 0.05$). All the results were represented corresponding to FDR multiple comparison correction with threshold $p < 0.05$. In contrast, the HC group showed no significant associations between hearing assessments, metabolite levels, dFNC, and cognitive function.

3.5 | Interactions Among Hearing Assessment, E/I-R, dFNC, and Cognition

As shown in the model (Figure 5A), the total effect of E/I-R on AVLT scores was statistically significant [total effect: $\beta = -1.7640$, $p < 0.001$, 95% confidence interval (CI) $(-2.5632, -0.9647)$], after controlling for sex ($\beta = 0.4677$, $p = 0.8227$), age ($\beta = -0.1796$, $p = 0.5593$), and education ($\beta = 0.3169$, $p = 0.4375$). When breaking down the total effect, the direct effect of E/I-R on AVLT scores was still significant [direct effect: $\beta' = -1.3184$, $p = 0.0019$, 95% CI $(-2.1390, -0.4978)$], and statistical significance was observed for the indirect effect of fractional windows in State 3 [indirect effect: $\Delta\beta = -0.4455$, 95% CI $(-0.9138, -0.1482)$]. Meanwhile, the mediation

percentage of the fractional windows in State 3 from E/I-R to AVLT was 0.25.

When the mediator was changed from the fractional windows to the dwell time in State 3 (Figure 5B), the mediation model was still valid. The total effect of E/I-R on AVLT scores was statistically significant [total effect: $\beta = -1.7640$, $p < 0.001$, 95% CI $(-2.5632, -0.9647)$] after controlling for the individual variables sex ($\beta = 0.4677$, $p = 0.8227$), age ($\beta = -0.1796$, $p = 0.5593$), and education ($\beta = 0.3169$, $p = 0.4375$). When breaking down the total effect, the direct effect of E/I-R on AVLT scores was still significant [direct effect: $\beta' = -1.4059$, $p = 0.0011$, 95% CI $(-2.23320, -0.5786)$]. Statistical significance was also observed for the indirect effect through fractional windows in State 3 [indirect effect: $\Delta\beta = -0.3580$, 95% CI $(-0.7569, -0.0812)$]. Meanwhile, the mediation percentage of the dwell time in State 3 from E/I-R to AVLT was 0.20.

Partial mediation was observed in the two models mentioned above, with the negative direct effect decreasing with respect to the total effect and the indirect effect being negative. In other words, when the effect fractional windows or dwell time in State 3 was isolated, the relationship between E/I-R and AVLT scores

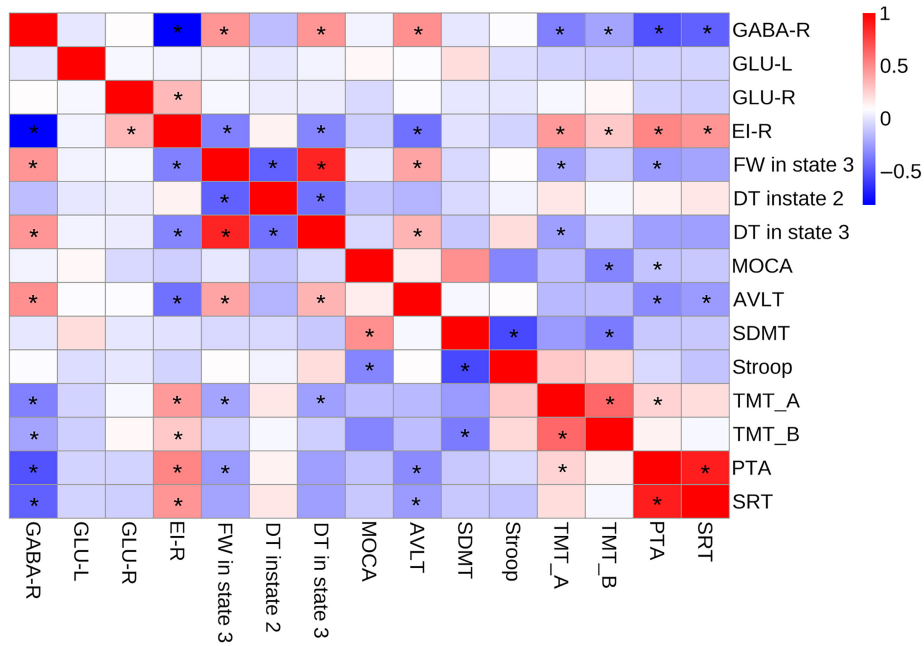


FIGURE 4 | Heatmap showing the correlation of among hearing assessment, E/I-R, dFNC, and cognition. DT: dwell time, E/I-R: E/I balance in the right auditory region, FW: fractional windows, GABA-R: GABA level in the right auditory region, GLU-L: GLU level in the left auditory region, GLU-R: GLU level in the right auditory region. * $p < 0.05$.

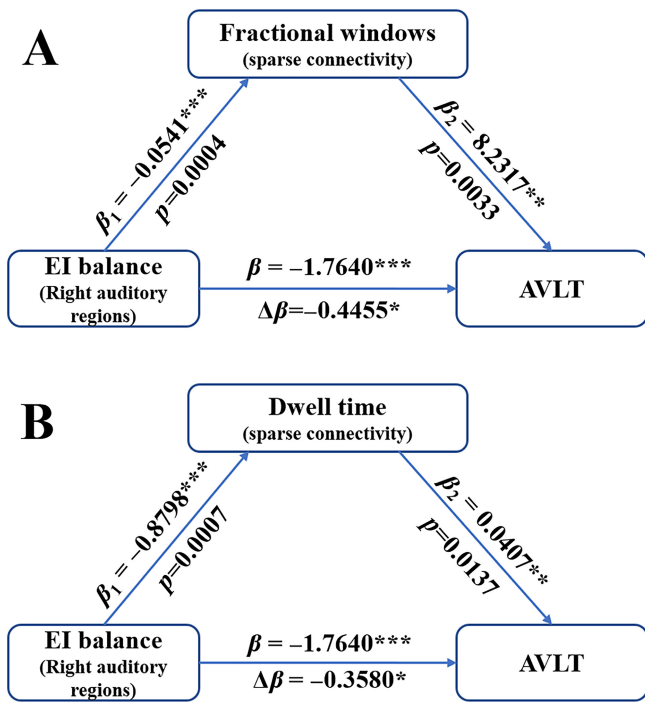


FIGURE 5 | Simple mediation models show the correlation between E/I balance in right auditory cortex and AVLT with fractional windows or dwell time as mediator. AVLT: Auditory Verbal Learning Test, E/I: excitation-inhibition. *** $p < 0.001$, ** $p < 0.01$, * $p < 0.05$.

was negative; however, in cases that presented a high fractional windows or dwell time in State 3, a negative effect on AVLT scores was observed.

In the serial mediation model (Figure 6A), PTA correlated with AVLT scores along four pathways. There was no statistically

significant direct effect of PTA on AVLT scores, indicating that the relationship between these two variables was not significant [direct effect: $\beta' = -0.1190$, $p = 0.2905$, 95% CI $(-0.3414, 0.1033)$]. Second, the relationship between PTA and AVLT scores through E/I-R was significant [$\beta_1 \times \beta_5 = -0.1397$, 95% CI $(-0.3587, -0.0680)$], but the relationship between PTA and AVLT scores through fractional windows in State 3 was not significant [$\beta_4 \times \beta_3 = -0.0265$, 95% CI $(-0.1069, 0.0388)$]. Finally, the serial indirect effect of E/I-R and fractional windows in State 3 was significant [$\beta_1 \times \beta_2 \times \beta_3 = -0.0489$, 95% CI $(-0.1047, -0.0096)$]. PTA exerted a statistically significant total effect on AVLT scores [total effect: $\beta = -0.3341$, $p = 0.0016$, 95% CI $(-0.5380, -0.1302)$], and the total indirect effect [$\beta_1 \times \beta_5 + \beta_1 \times \beta_2 \times \beta_3 + \beta_4 \times \beta_3 = -0.2151$, 95% CI $(-0.3587, -0.0680)$] was statistically significant. Meanwhile, the mediation percentage of E/I-R and the fractional windows in State 3 from PTA to AVLT was 0.64.

When the mediator was changed from the fractional windows to dwell time in State 3 (Figure 6B), the mediation model was still valid. Again, there was no significant direct effect from PTA to AVLT scores. [direct effect: $\beta' = -0.1288$, $p = 0.2584$, 95% CI $(-0.3538, 0.0962)$]. Second, the relationship between PTA and AVLT scores through E/I-R was significant [$\beta_1 \times \beta_5 = -0.1435$, 95% CI $(-0.3406, -0.0597)$], although the relationship between PTA and AVLT scores through dwell time in State 3 was not significant [$\beta_4 \times \beta_3 = -0.0162$, 95% CI $(-0.0739, 0.0350)$]. Finally, the serial indirect effect of E/I-R and fractional windows in State 3 was significant [$\beta_1 \times \beta_2 \times \beta_3 = -0.0394$, 95% CI $(-0.0887, -0.0051)$]. The significant total effect of PTA on AVLT scores was unchanged [total effect: $\beta = -0.3341$, $p = 0.0016$, 95% CI $(-0.5380, -0.1302)$], although the total indirect effect [$\beta_1 \times \beta_5 + \beta_1 \times \beta_2 \times \beta_3 + \beta_4 \times \beta_3 = -0.2053$, 95% CI $(-0.3481, -0.0624)$] was statistically significant. Meanwhile, the mediation percentage of E/I-R and the dwell time in State 3 from PTA to AVLT was 0.61.

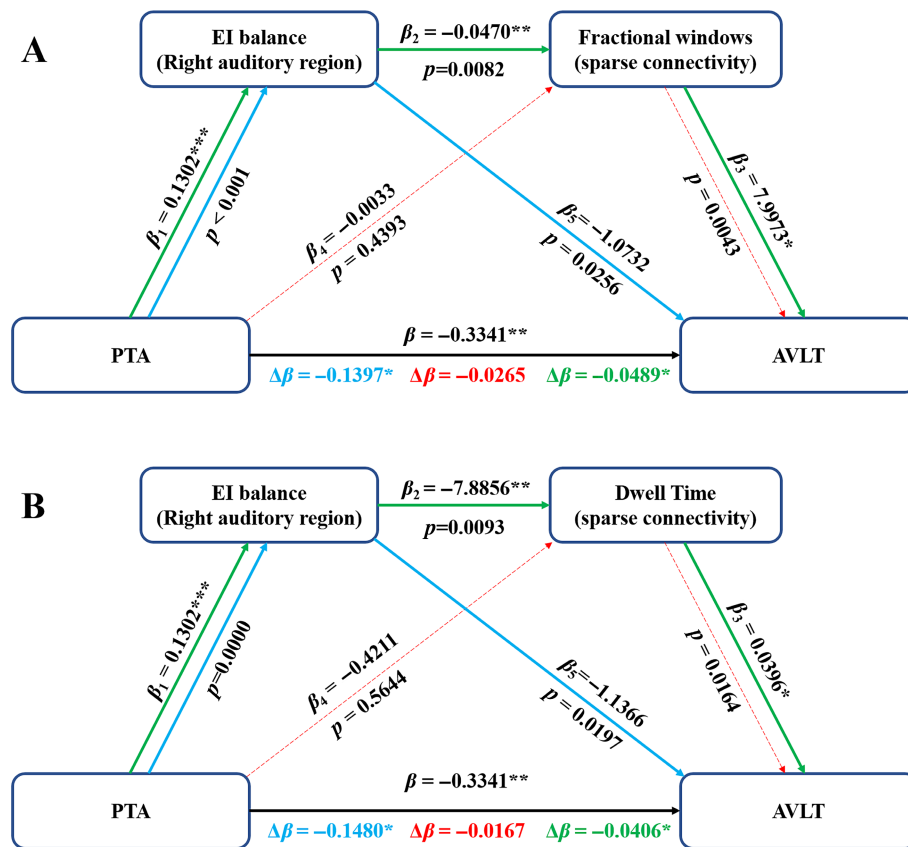


FIGURE 6 | Serial mediation models show the correlation among PTA, E/I balance in right auditory cortex, fractional windows/dwell time, and AVLTL. AVLTL: Auditory Verbal Learning Test, EI: excitation–inhibition, PTA: pure tone average. *** $p < 0.001$, ** $p < 0.01$, * $p < 0.05$.

Partial mediation was observed in the two serial mediation models mentioned above. In patients with presbycusis, worse hearing ability contribute to lower GABA, higher E/I balance, and further impact aberrant dFNC, which caused lower AVLTL scores.

4 | Discussion

This investigation delved into the connections between hearing loss, regional neurotransmitter concentrations, time-varying functional connectivity, and changes in cognition in presbycusis. The main results were as follows: (1) lower GABA levels in right Heschl's gyri and Glu levels in bilateral Heschl's gyri but higher E/I balance in right Heschl's gyri in presbycusis; (2) discernible alterations in dynamic functional connectivity in presbycusis patients; and (3) the mediation of the relationship between PTA and AVLTL by the right auditory E/I balance and fractional windows/dwell time in state of sparse connectivity.

4.1 | Altered Auditory E/I Balance in Presbycusis

GABA plays a pivotal role in the processing of acoustic information within the human nervous system. In this study, we revealed a significant reduction in right auditory GABA levels and bilateral auditory Glu levels in presbycusis patient. Notably, this

finding is consistent with the previous research (Gao et al. 2015; Li et al. 2023). To further explore metabolic changes, we used the E/I balance (measured by the Glu/GABA ratio). Various distinctive features—including reduced GABA release, decline in the number of GABA neurons, reduced GABA levels, and decreased concentration of glutamic acid decarboxylase (GAD) within the auditory gyri—have been reported in animal models of presbycusis (Burianova et al. 2009; Syka 2010), all of which reflect disruptions in GABAergic neurotransmission. Another study reported lower auditory GABA levels in older compared to younger participants, and that the GABA level in the right auditory cortex mediated the relationship between age and sound-in-noise understanding loss (Dobri and Ross 2021). Likewise, lower Glu concentrations in older rats relative to younger rats have been reported throughout central auditory areas (Godfrey et al. 2017). Lower Glu levels have also been reported in elderly people with presbycusis in bilateral Heschl's gyrus (Profant et al. 2013). Although some studies did not use elderly health participants as a control group to make sure the above changes are due to hearing loss not aging, we think decreased GABA and/or Glu levels may disrupt the E/I balance in presbycusis, as supported by our finding that E/I balance was significantly decreased in the right auditory area in the PC group. It is reasonable that E/I balance moves toward excitation when the number of meaningful stimuli is reduced in patients with presbycusis in partial hearing deprivation situations, which is consistent with findings from an experiment with rats (Žiburkus, Cressman, and Schiff 2013).

4.2 | Altered Dynamic Functional Connectivity in Presbycusis Patients

Patients with presbycusis have different time-varying characteristics compared to HCs. The varied temporal characteristics of dFNC suggest flexibility in functional coordination between brain networks. State 1, mainly manifesting as negative connectivity between SN (IC21) and VN (IC71), SMN (IC78), and positive correlations between VN and SMN, AN and SMN, DMN, showed minimum occurrences (81/158). State 2, which was mainly characterized as positive connectivity and represents high and strong interconnection with intra- and inter-brain networks, was the most frequent brain state in the HC group and had a higher probability of transitioning. In contrast, State 3, which presented as sparse connectivity representing segregated brain networks, appeared most frequently in the PC group. More fractional windows and longer mean dwell time in sparse connectivity were associated with worse cognitive ability, indicating reduced crosstalk between brain networks, more unstable network connectivity, more inefficient functional integration, and lower fluency in brain cognitive resource allocation (Kim et al. 2017; Xing et al. 2022).

4.3 | Reorganization in Cognitive-Ear Link Resulted by Hearing Deprivation in Patients With Presbycusis

It is well-established that hearing loss is an independent risk factor for dementia and may contribute to the development of Alzheimer's disease (AD) (Livingston et al. 2017; Panza, Solfrizzi, and Logroscino 2015). Sensory deprivation theory, mainly focused on auditory deprivation, provides an explanation of the neural mechanisms underlying the cognition-ear link in presbycusis. Despite our earnest efforts to clarify alterations in the neural system and their association with cognitive decline, there are still numerous unexplored areas ripe for investigation. Through sequential mediation model analyses, we discerned that right auditory E/I balance and temporal properties of dynamic functional connectivity states mediated the correlation between hearing loss and cognitive impairment. It is clear from the previous study that in patients with presbycusis, right auditory GABA levels are closely correlated with hearing loss (Gao et al. 2015; Li et al. 2023). Nevertheless, the combination of Glu-mediated excitation and GABA-mediated inhibition can furnish more robust evidence to enhance understanding of the neural systems responsible for processing sensory information, diverse forms of memory, and social and emotional behaviors. E/I balance, which is regulated by plastic neural synapses and regulates the activity of neural networks in turn, is dynamic during the morphological and functional development of cerebral cortical tissue (Benítez-Díaz et al. 2006) and the period from adolescence to adulthood (Perica et al. 2022). In a study of mice, with progressive hearing loss, expression of GABA and Glu receptors were significantly altered in areas such as the hippocampus and auditory cortex, implying extensive reorganization of plasticity-related neurotransmitter expression (Beckmann et al. 2020). These findings indicate that hearing loss may disrupt E/I balance in the right auditory cortex and support our mediation model of the relationship between PTA and E/I balance.

Excitatory and inhibitory neurotransmitters play important roles in various neurobiological processes including cellular proliferation, migration, differentiation, synaptogenesis, and local circuit maturation (Benítez-Díaz et al. 2006; Howes and Shatalina 2022). Lower GABA levels may exert an impact on auditory synaptic plasticity (Casparly et al. 2008). E/I balance has emerged as a pivotal determinant of the stability of the network, comprising three-layers of spiking neurons corresponding to the skin, subcortical, and cortical structures (Xing and Gerstein 1996). Rădulescu et al. demonstrated that subtle shifts in the relative strength of E/I of medium spiny neurons expressing D1 or D2 dopamine receptors powerfully control the network dynamics of the cortico-striatal-thalamo-cortical pathway in ways that are not easily predicted solely by synaptic connections using nonlinear modeling of neuronal activity and bifurcation theory in their computational model (Rădulescu et al. 2017). Not only does E/I balance participate in instantaneous regulation of neural activity, it is also related to long-term potentiation (LTP)-like plasticity, which could influence learning and memory (Wijtenburg et al. 2017). Another study reported that the amount of GABAergic excitation was increased in suprachiasmatic nucleus (SCN) slices of old mice and that the E/I balance was higher compared to young controls, suggesting potential contributions to altered synchrony within the aged SCN network through changes in GABAergic function (Olde Engberink et al. 2023). Adaptation memory, that is, after-effect retention, may also increase with age owing to an age-related GABA decline and increased E/I ratio in the primary motor cortex (Xing et al. 2021), suggesting LTP in the human sensorimotor cortex. Although there are no reports of the relationship between E/I balance and dFNC so far, the effect of E/I balance on cellular electrophysiological changes and oscillation in brain networks provide evidence for our mediation model, indicating compensation of whole-brain dFNC driven by E/I-R in presbycusis patients.

Recent studies have reported that changes in dFNC are closely related to complex cognitive functions in neurodegenerative disorders and other, often untreatable conditions, such as AD (Quevenco et al. 2019), PD (Fiorenzato et al. 2019; Kim et al. 2017), PC (Xing et al. 2023, 2021), and multiple sclerosis (MS) (Schoonheim et al. 2021), involving multiple network connectivity SN, CB, AN, VN, SMN, DMN, and CEN. Although there was no group difference in the connectivity strength of each state at various regional pairings in our study, changes in time-varying characteristics were detected in presbycusis patients. Increased fractional windows and dwell time in sparse connectivity between functional networks were positively correlated with total AVLT scores, which reflect verbal learning and memory of supra-span lists of words. As commonly acknowledged, the human brain dynamically reconfigures segregation and integration to facilitate a wide range of cognitive tasks, with particular emphasis on enhanced integration during tasks requiring substantial cognitive load (Wang et al. 2021). Based on the sensory deprivation hypothesis of the cognition-ear link (Lozupone, Sardone, and Panza 2020), PC patients may recruit more cognitive resources to support episodic memory (Marcotte and Ansaldo 2014; Soch et al. 2022). Thus, the relationship between dFNC change and cognition decline may mirror the presence of maladaptive exhaustion of inter-network compensatory mechanisms.

In the simple mediation analysis, the fractional windows and dwell time in sparse dFNC mediated the link between E/I-Rand total AVLT scores. There is evidence that dFNC of the cerebellum with the auditory and visual networks is decreased in PC patients (Xing et al. 2022), increased resting-state FNC of the anterior DMN and anterior insula (Li et al. 2023), and that large-scale distributed neural circuits undergo dynamic reconfiguration during executive cognition in communication of the DMN with task-positive networks, namely the frontoparietal and subcortical systems (Braun et al. 2015; Finc et al. 2020). After using GABA_A receptor antagonist in a rat experiment, notable alterations were observed in resting-state BOLD activation both within and between the somatosensory and visual cortices, alongside the caudate putamen; this study also demonstrated a consistent correlation with resting EEG coherence in the alpha and beta frequency bands (Nasrallah et al. 2017). Above all, an increased E/I ratio in the right auditory cortex may trigger a change in network connectivity among the auditory cortex and other functional areas, leading to increased AVLT scores. Notably, there was also a direct effect of E/I balance on AVLT scores. A Cntnap2 knockout mice study suggested that a lower prefrontal cortex Glu/GABA ratio along with changes in other metabolites might contribute to social behavior deficits (Park et al. 2022). It is reasonable that cognition and behavior are affected by disrupted E/I balance, both in excessive excitatory and inhibitory states. In summary, in cases of hearing loss, a shifted E/I balance toward excitation and decreased fractional windows and dwell time in sparse network connectivity may lead to cognitive impairment. The serial mediation models indicated that hearing loss can affect cognition via a bottom-up route from ear to cognition via neurochemicals and dFNC, supporting reorganization of the cognition-ear link under partial hearing deprivation in patients with presbycusis.

4.4 | Limitations

This study is not without its limitations. Firstly, as a cross-sectional study, there are inherent constraints in establishing causal relationships from the observed correlations. To address this limitation, future research should adopt a longitudinal design to assess changes in neurochemistry and dFNC in relation to cognitive impairment in presbycusis. Secondly, the transient dFNC patterns, which are essentially connectivity strengths between different states and regional pairings, did not yield statistically significant findings. With the method of cross-validation, internal (leave one out or e.g. 5-fold), and/or external (to another dataset), we can utilize Group ICA to achieve supervised learning, which may better distinguish the differences in brain networks between patients with presbycusis and health controls. Thirdly, it is challenging to measure the whole-brain E/I ratio in MRS analysis and we lacked a control VOI. Moreover, the shifted E/I balance toward excitation in right auditory cortex or at whole-brain level remains unknown. Thus, more in-depth research on neurochemical and dFNC reorganization under partial hearing deprivation in presbycusis is warranted.

4.5 | Conclusion

Overall, this study presents a comprehensive examination of presbycusis patients, revealing a noticeable shift in the E/I

balance and marked changes in the temporal characteristics of dFNC. These alterations were closely intertwined with both auditory and cognitive impairment, which provide evidence for the impact of sensory deprivation. The E/I ratio, along with the reduced fractional windows and dwell time in sparse dFNC, mediated the correlation between hearing loss and episodic verbal learning and recall abilities in presbycusis patients, suggesting that neurochemical metabolites and dFNC play important roles in the potential pathway from hearing to cognition. Importantly, E/I balance, which is affected by hearing loss and directly regulates brain network connectivity associated with cognitive impairment, plays an essential role in reorganization of the cognition-ear relationship. These findings greatly facilitate our comprehension of the relationship between neural mechanisms and cognitive impairment in individuals with presbycusis. Consequently, E/I balance hold promise as potential biomarkers for investigating and predicting cognitive impairment. Even, with above findings, it is promising that improving hearing or using drugs to alter the concentration of metabolite GABA and further affect E/I balance may maintain or even improve cognition in elderly deaf patients.

Acknowledgements

This work was supported by the National Natural Science Foundation of China (No. 81601479); Taishan Scholars Project of Shandong Province (No. tstp20240525); Shandong Provincial Natural Science Foundation of China (Grants ZR2021MH030, ZR2021MH355), the Academic Promotion Programme of Shandong First Medical University (Grant 2019QL023) and Postdoctoral Innovation Projects of Shandong Province (No. SDCX-ZG-202400047). This work was also supported by National Institutes of Health (Grants R01 EB016089, R01 EB023963, R21 AG060245, P41 EB015909, and P41 EB031771).

Conflicts of Interest

The authors declare no conflicts of interest.

Data Availability Statement

The data that support the findings of this study are available from the corresponding author upon reasonable request.

References

- Albers, M. W., G. C. Gilmore, J. Kaye, et al. 2015. "At the Interface of Sensory and Motor Dysfunctions and Alzheimer's Disease." *Alzheimer's & Dementia* 1: 70–98.
- Allen, E. A., E. Damaraju, S. M. Plis, E. B. Erhardt, T. Eichele, and V. D. Calhoun. 2014. "Tracking Whole-Brain Connectivity Dynamics in the Resting State." *Cerebral Cortex* 24, no. 3: 663–676.
- Bartos, M., I. Vida, and P. Jonas. 2007. "Synaptic Mechanisms of Synchronized Gamma Oscillations in Inhibitory Interneuron Networks." *Nature Reviews. Neuroscience* 8, no. 1: 45–56. <https://doi.org/10.1038/nrn2044>.
- Beckmann, D., M. Feldmann, O. Shchyglo, and D. Manahan-Vaughan. 2020. "Hippocampal Synaptic Plasticity, Spatial Memory, and Neurotransmitter Receptor Expression Are Profoundly Altered by Gradual Loss of Hearing Ability." *Cerebral Cortex* 30, no. 8: 4581–4596.
- Belkhiria, C., R. C. Vergara, S. San Martin, et al. 2020. "Insula and Amygdala Atrophy Are Associated With Functional Impairment in Subjects With Presbycusis." *Frontiers in Aging Neuroscience* 12: 102. <https://doi.org/10.3389/fnagi.2020.00102>.

- Benítez-Díaz, P., L. Miranda-Contreras, Z. Peña-Contreras, D. Dávila-Vera, R. V. Mendoza-Briceno, and E. Palacios-Prü. 2006. "Histotypic Mouse Parietal Cortex Cultures: Excitation/Inhibition Ratio and Ultrastructural Analysis." *Journal of Neuroscience Methods* 156, no. 1-2: 64–70.
- Braun, U., A. Schäfer, H. Walter, et al. 2015. "Dynamic Reconfiguration of Frontal Brain Networks During Executive Cognition in Humans." *Proceedings of the National Academy of Sciences* 112, no. 37: 11678–11683.
- Burianova, J., L. Ouda, O. Profant, and J. Syka. 2009. "Age-Related Changes in GAD Levels in the Central Auditory System of the Rat." *Experimental Gerontology* 44, no. 3: 161–169.
- Calhoun, V. D., T. Adali, G. D. Pearlson, and J. J. Pekar. 2001. "A Method for Making Group Inferences From Functional MRI Data Using Independent Component Analysis." *Human Brain Mapping* 14, no. 3: 140–151.
- Casparly, D. M., L. Ling, J. G. Turner, and L. F. Hughes. 2008. "Inhibitory Neurotransmission, Plasticity and Aging in the Mammalian Central Auditory System." *Journal of Experimental Biology* 211, no. 11: 1781–1791.
- Casparly, D., A. Raza, B. L. Armour, J. Pippin, and S. Arneric. 1990. "Immunocytochemical and Neurochemical Evidence for Age-Related Loss of GABA in the Inferior Colliculus: Implications for Neural Presbycusis." *Journal of Neuroscience* 10, no. 7: 2363–2372.
- Chang, C., and G. H. Glover. 2010. "Time–Frequency Dynamics of Resting-State Brain Connectivity Measured With fMRI." *NeuroImage* 50, no. 1: 81–98.
- Chao-Gan, W., X.-N. Xin-Di, and Z. Yu-Feng. 2016. "DPABI: Data Processing & Analysis for (Resting-State) Brain Imaging." *Neuroinformatics* 14, no. 3: 339–351.
- Chen, J. E., M. Rubinov, and C. Chang. 2017. "Methods and Considerations for Dynamic Analysis of Functional MR Imaging Data." *Neuroimaging Clinics of North America* 27: 547–560.
- Chen, Y. C., W. Yong, C. Xing, Y. Feng, and Y. Wu. 2019. "Directed Functional Connectivity of the Hippocampus in Patients With Presbycusis." *Brain Imaging and Behavior* 14, no. 4: 917–926.
- Damaraju, E., E. A. Allen, A. Belger, et al. 2014. "Dynamic Functional Connectivity Analysis Reveals Transient States of Dysconnectivity in Schizophrenia." *NeuroImage: Clinical* 5: 298–308.
- Dobri, S. G., and B. Ross. 2021. "Total GABA Level in Human Auditory Cortex Is Associated With Speech-in-Noise Understanding in Older Age." *NeuroImage* 225: 117474.
- Edden, R. A., J. Intrapiromkul, H. Zhu, Y. Cheng, and P. B. Barker. 2012. "Measuring T2 In Vivo With J-Difference Editing: Application to GABA at 3 Tesla." *Journal of Magnetic Resonance Imaging* 35, no. 1: 229–234. <https://doi.org/10.1002/jmri.22865>.
- Edden, R. A., N. A. Puts, A. D. Harris, P. B. Barker, and C. J. Evans. 2014. "Gannet: A Batch-Processing Tool for the Quantitative Analysis of Gamma-Aminobutyric Acid-Edited MR Spectroscopy Spectra." *Journal of Magnetic Resonance Imaging* 40, no. 6: 1445–1452. <https://doi.org/10.1002/jmri.24478>.
- Finc, K., K. Bonna, X. He, et al. 2020. "Dynamic Reconfiguration of Functional Brain Networks During Working Memory Training." *Nature Communications* 11, no. 1: 2435.
- Fiorenzato, E., A. P. Strafella, J. Kim, R. Schifano, and R. Biundo. 2019. "Dynamic Functional Connectivity Changes Associated With Dementia in Parkinson's Disease." *Brain* 142, no. 9: 2860–2872.
- Ganji, S. K., A. Banerjee, A. M. Patel, et al. 2012. "T2 Measurement of J-Coupled Metabolites in the Human Brain at 3T." *NMR in Biomedicine* 25, no. 4: 523–529. <https://doi.org/10.1002/nbm.1767>.
- Gao, F., G. Wang, W. Ma, et al. 2015. "Decreased Auditory GABA+ Concentrations in Presbycusis Demonstrated by Edited Magnetic Resonance Spectroscopy." *NeuroImage* 106: 311–316.
- Gasparovic, C., T. Song, D. Devier, et al. 2006. "Use of Tissue Water as a Concentration Reference for Proton Spectroscopic Imaging." *Magnetic Resonance in Medicine* 55, no. 6: 1219–1226. <https://doi.org/10.1002/mrm.20901>.
- Gates, G. A., and J. H. Mills. 2005. "Presbycusis." *Lancet* 366, no. 9491: 1111–1120.
- Godfrey, D. A., K. Chen, T. R. O'Toole, and A. I. Mustapha. 2017. "Amino Acid and Acetylcholine Chemistry in the Central Auditory System of Young, Middle-Aged and Old Rats." *Hearing Research* 350: 173–188.
- Harris, A. D., N. A. J. Puts, P. B. Barker, and R. A. E. Edden. 2015. "Spectral-Editing Measurements of GABA in the Human Brain With and Without Macromolecule Suppression." *Magnetic Resonance in Medicine* 74: 1523–1529.
- Hayes, A. F. 2017. *Introduction to Mediation, Moderation, and Conditional Process Analysis: A Regression-Based Approach*. New York: The Guilford Press.
- Howes, O. D., and E. Shatalina. 2022. "Integrating the Neurodevelopmental and Dopamine Hypotheses of Schizophrenia and the Role of Cortical Excitation-Inhibition Balance." *Biological Psychiatry* 92, no. 6: 501–513.
- Karl, J., S. Williams, R. Howard, R. Frackowiak, and R. Turner. 1996. "Movement-Related Effects in fMRI Time-Series." *Magnetic Resonance in Medicine* 35, no. 3: 346–355.
- Kim, J., M. Criaud, S. S. Cho, et al. 2017. "Abnormal Intrinsic Brain Functional Network Dynamics in Parkinson's Disease." *Brain* 11, no. 11: 2955–2967.
- Lalwani, P., H. Gagnon, K. E. Cassady, et al. 2019. "Neural Distinctiveness Declines With Age in Auditory Cortex and Is Associated With Auditory GABA Levels." *NeuroImage* 201: 116033. <https://doi.org/10.1016/j.neuroimage.2019.116033>.
- Leonardi, N., and D. Van De Ville. 2015. "On Spurious and Real Fluctuations of Dynamic Functional Connectivity During Rest." *NeuroImage* 104: 430–436.
- Li, N., W. Ma, F. Ren, et al. 2023. "Neurochemical and Functional Reorganization of the Cognitive-Ear Link Underlies Cognitive Impairment in Presbycusis." *NeuroImage* 268: 119861.
- Lin, F. R., and M. Albert. 2014. "Hearing Loss and Dementia—Who Is Listening?" *Aging & Mental Health* 18, no. 6: 671–673.
- Lin, F. R., T. Roland, G. S. Sandra, and F. Luigi. 2011. "Hearing Loss Prevalence and Risk Factors Among Older Adults in the United States." *Journal of Gerontology* 5: 582–590.
- Livingston, G., A. Sommerlad, V. Orgeta, et al. 2017. "Dementia Prevention, Intervention, and Care." *Lancet* 390, no. 10113: 2673–2734.
- Loughrey, D. G., M. E. Kelly, G. A. Kelley, S. Brennan, and B. A. Lawlor. 2018. "Association of Age-Related Hearing Loss With Cognitive Function, Cognitive Impairment, and Dementia: A Systematic Review and Meta-Analysis." *Jama Otolaryngology—Head & Neck Surgery* 144, no. 2: 115–126. <https://doi.org/10.1001/jamaoto.2017.2513>.
- Lozupone, M., R. Sardone, and F. Panza. 2020. "Age-Related Hearing Loss and Neuropathologic Burden: A Step Inside the Cognitive Ear." *Neurology* 95, no. 12: 511–512. <https://doi.org/10.1212/WNL.0000000000010580>.
- Lu, H., L. M. Nagae-Poetscher, X. Golay, D. Lin, M. Pomper, and P. C. van Zijl. 2005. "Routine Clinical Brain MRI Sequences for Use at 3.0 Tesla." *Journal of Magnetic Resonance Imaging* 22, no. 1: 13–22. <https://doi.org/10.1002/jmri.20356>.
- Lu, J., D. Li, F. Li, et al. 2011. "Montreal Cognitive Assessment in Detecting Cognitive Impairment in Chinese Elderly Individuals: A Population-Based Study." *Journal of Geriatric Psychiatry and Neurology* 24, no. 4: 184–190.

- Marcotte, K., and A. I. Ansaldo. 2014. "Age-Related Behavioural and Neurofunctional Patterns of Second Language Word Learning: Different Ways of Being Successful." *Brain and Language* 135: 9–19.
- Mlynarik, V., S. Gruber, and E. Moser. 2001. "Proton T₁ and T₂ Relaxation Times of Human Brain Metabolites at 3 Tesla." *NMR in Biomedicine* 14, no. 5: 325–331.
- Mullins, P. G., D. J. McGonigle, R. L. O'Gorman, et al. 2014. "Current Practice in the Use of MEGA-PRESS Spectroscopy for the Detection of GABA." *NeuroImage* 86: 43–52. <https://doi.org/10.1016/j.neuroimage.2012.12.004>.
- Nasrallah, F. A., K. Kaur, O. R. Singh, L. Y. Yeow, and K.-H. Chuang. 2017. "GABAergic Effect on Resting-State Functional Connectivity: Dynamics Under Pharmacological Antagonism." *NeuroImage* 149: 53–62.
- Olde Engberink, A. H., P. de Torres Gutiérrez, A. Chiosso, A. Das, J. H. Meijer, and S. Michel. 2023. "Aging Affects GABAergic Function and Calcium Homeostasis in the Mammalian Central Clock." *Frontiers in Neuroscience* 17: 1178457.
- Panza, F., V. Solfrizzi, and G. Logroscino. 2015. "Age-Related Hearing Impairment—A Risk Factor and Frailty Marker for Dementia and AD." *Nature Reviews Neurology* 11, no. 3: 166–175.
- Park, G., S. J. Jeon, I. O. Ko, et al. 2022. "Decreased In Vivo Glutamate/GABA Ratio Correlates With the Social Behavior Deficit in a Mouse Model of Autism Spectrum Disorder." *Molecular Brain* 15, no. 1: 1–12.
- Perica, M. I., F. J. Calabro, B. Larsen, et al. 2022. "Development of Frontal GABA and Glutamate Supports Excitation/Inhibition Balance From Adolescence Into Adulthood." *Progress in Neurobiology* 219: 102370.
- Piechnik, S. K., J. Evans, L. H. Bary, R. G. Wise, and P. Jezzard. 2009. "Functional Changes in CSF Volume Estimated Using Measurement of Water T2 Relaxation." *Magnetic Resonance in Medicine* 61, no. 3: 579–586. <https://doi.org/10.1002/mrm.21897>.
- Profant, O., Z. Balogová, M. Dezortová, D. Wagnerová, M. Hájek, and J. Syka. 2013. "Metabolic Changes in the Auditory Cortex in Presbycusis Demonstrated by MR Spectroscopy." *Experimental Gerontology* 48, no. 8: 795–800.
- Provencher, S. W. 1993. "Estimation of Metabolite Concentrations From Localized In Vivo Proton NMR Spectra." *Magnetic Resonance in Medicine* 30, no. 6: 672–679.
- Puts, N. A., P. B. Barker, and R. A. Edden. 2013. "Measuring the Longitudinal Relaxation Time of GABA In Vivo at 3 Tesla." *Journal of Magnetic Resonance Imaging* 37, no. 4: 999–1003. <https://doi.org/10.1002/jmri.23817>.
- Qian, Z. J., P. D. Chang, G. Moonis, and A. K. Lalwani. 2017. "A Novel Method of Quantifying Brain Atrophy Associated With Age-Related Hearing Loss." *Neuroimage: Clinical* 16: 205–209.
- Quevenco, F. C., S. J. Schreiner, M. G. Preti, et al. 2019. "GABA and Glutamate Moderate Beta-Amyloid Related Functional Connectivity in Cognitively Unimpaired Old-Aged Adults." *NeuroImage: Clinical* 22: 101776.
- Rădulescu, A., J. Herron, C. Kennedy, and A. Scimemi. 2017. "Global and Local Excitation and Inhibition Shape the Dynamics of the Cortico-Striatal-Thalamo-Cortical Pathway." *Scientific Reports* 7, no. 1: 7608.
- Sakoğlu, Ü., G. D. Pearlson, K. A. Kiehl, Y. M. Wang, A. M. Michael, and V. D. Calhoun. 2010. "A Method for Evaluating Dynamic Functional Network Connectivity and Task-Modulation: Application to Schizophrenia." *Magnetic Resonance Materials in Physics, Biology and Medicine* 23: 351–366.
- Sánchez-Cubillo, I., J. A. Periáñez, D. Adrover-Roig, et al. 2009. "Construct Validity of the Trail Making Test: Role of Task-Switching, Working Memory, Inhibition/Interference Control, and Visuomotor Abilities." *Journal of the International Neuropsychological Society* 15, no. 3: 438–450.
- Savitz, J., and P. Jansen. 2003. "The Stroop Color-Word Interference Test as an Indicator of ADHD in Poor Readers." *Journal of Genetic Psychology* 164, no. 3: 319–333.
- Schependom, J. V., M. B. D'Hooghe, K. Cleyhens, et al. 2014. "The Symbol Digit Modalities Test as Sentinel Test for Cognitive Impairment in Multiple Sclerosis." *European Journal of Neurology* 21: 1219.
- Schoonheim, M. M., L. Douw, T. A. Broeders, A. J. Eijlers, K. A. Meijer, and J. J. Geurts. 2021. "The Cerebellum and Its Network: Disrupted Static and Dynamic Functional Connectivity Patterns and Cognitive Impairment in Multiple Sclerosis." *Multiple Sclerosis Journal* 27, no. 13: 2031–2039.
- Schulte, A., C. M. Thiel, A. Gieseler, M. Tahden, H. Colonius, and S. Rosemann. 2020. "Reduced Resting State Functional Connectivity With Increasing Age-Related Hearing Loss and McGurk Susceptibility." *Scientific Reports* 10, no. 1: 16987.
- Shirer, W. R., S. Ryali, E. Rykhlevskaia, V. Menon, and M. D. Greicius. 2012. "Decoding Subject-Driven Cognitive States With Whole-Brain Connectivity Patterns." *Cerebral Cortex* 22, no. 1: 158–165. <https://doi.org/10.1093/cercor/bhr099>.
- Soch, J., A. Richter, J. M. Kizilirmak, et al. 2022. "Structural and Functional MRI Data Differentially Predict Chronological Age and Behavioral Memory Performance." *ENeuro* 9, no. 6: ENEURO.0212-22.2022.
- Syka, J. 2010. "The Fischer 344 Rat as a Model of Presbycusis." *Hearing Research* 264, no. 1-2: 70–78.
- Tang, X., X. Zhu, B. Ding, J. P. Walton, R. D. Frisina, and J. Su. 2014. "Age-Related Hearing Loss: GABA, Nicotinic Acetylcholine and NMDA Receptor Expression Changes in Spiral Ganglion Neurons of the Mouse." *Neuroscience* 259: 184–193.
- Wang, R., M. Liu, X. Cheng, Y. Wu, A. Hildebrandt, and C. Zhou. 2021. "Segregation, Integration, and Balance of Large-Scale Resting Brain Networks Configure Different Cognitive Abilities." *Proceedings of the National Academy of Sciences* 118, no. 23: e2022288118.
- Wansapura, J. P., S. K. Holland, R. S. Dunn, and W. S. Ball Jr. 1999. "NMR Relaxation Times in the Human Brain at 3.0 Tesla." *Journal of Magnetic Resonance Imaging* 9, no. 4: 531–538.
- Wijtenburg, S. A., J. West, S. A. Korenic, et al. 2017. "Glutamatergic Metabolites Are Associated With Visual Plasticity in Humans." *Neuroscience Letters* 644: 30–36.
- Xie, H., C. Y. Zheng, D. A. Handwerker, et al. 2019. "Efficacy of Different Dynamic Functional Connectivity Methods to Capture Cognitively Relevant Information." *NeuroImage* 188: 502–514.
- Xing, C., W. Chang, Y. Liu, et al. 2023. "Alteration in Resting-State Effective Connectivity Within the Papez Circuit in Presbycusis." *European Journal of Neuroscience* 58: 3026–3036.
- Xing, C., Y.-C. Chen, J.-J. Xu, et al. 2021. "Abnormal Static and Dynamic Functional Network Connectivity in Patients With Presbycusis." *Frontiers in Aging Neuroscience* 13: 774901.
- Xing, C., Y.-C. Chen, S.a. Shang, et al. 2022. "Abnormal Static and Dynamic Functional Network Connectivity in Patients With Presbycusis." *Frontiers in Aging Neuroscience* 13: 774901.
- Xing, J., and G. L. Gerstein. 1996. "Networks With Lateral Connectivity. I. Dynamic Properties Mediated by the Balance of Intrinsic Excitation and Inhibition." *Journal of Neurophysiology* 75, no. 1: 184–199.
- Zhao, Q., Y. Lv, Y. Zhou, Z. Hong, and Q. Guo. 2012. "Short-Term Delayed Recall of Auditory Verbal Learning Test Is Equivalent to Long-Term Delayed Recall for Identifying Amnesic Mild Cognitive Impairment." *PLoS One* 7: e51157.

Zigmond, A. S., and R. P. Snaith. 1983. "The Hospital Anxiety and Depression Scale." *Acta Psychiatrica Scandinavica* 67, no. 6: 361–370.

Žiburkus, J., J. R. Cressman, and S. J. Schiff. 2013. "Seizures as Imbalanced Up States: Excitatory and Inhibitory Conductances During Seizure-Like Events." *Journal of Neurophysiology* 109, no. 5: 1296–1306.

Supporting Information

Additional supporting information can be found online in the Supporting Information section.